Technical Note

Effect of Overburden Stress and Plasticity on the Cyclic Resistance of Silts

Ali Dadashiserej[1]; Amalesh Jana, M.ASCE[2]; Armin W. Stuedlein, M.ASCE[3]; and T. Matthew Evans, M.ASCE[4]

Abstract: The effect of vertical effective consolidation stress, σ'_{vc}, on the cyclic resistance of nonplastic to plastic normally consolidated (NC) and overconsolidated (OC) intact and NC reconstituted silt was investigated using a series of constant-volume, stress-controlled cyclic direct simple shear (CDSS) tests. The results were interpreted considering the changes of specimen properties [e.g., void ratio, e, and overconsolidation ratio (OCR)] associated with the increased σ'_{vc}. Despite increasing density, all specimens exhibited a reduction in cyclic resistance as σ'_{vc} increased. The reduction in cyclic resistance for intact specimens occurred due to the detrimental effect of yielding of the natural soil fabric, reduction in OCR, and the potential suppression of dilative tendencies, which outweighed the beneficial effect of reduced e. Tests of uniformly prepared reconstituted NC specimens reduced the number of factors contributing to the reduction of cyclic resistance (i.e., destruction of natural soil fabric, and reduction of OCR) with increased σ'_{vc}, and were used to confirm the sensitivity of cyclic resistance to σ'_{vc}, in which the detrimental effect of suppressed dilative tendencies on cyclic resistance dominated the beneficial effect of reduced e. The overburden correction factor, K_σ, was observed to decrease with increased plasticity index, PI, highlighting the role of compressibility on cyclic resistance. **DOI: 10.1061/JGGEFK.GTENG-11345.**

Introduction

The effect of vertical effective overburden stress, σ'_{v0}, on the cyclic response of cohesionless soils commonly is addressed using the overburden correction factor, K_σ, introduced by Seed (1983). Increases in σ'_{v0} lead to the suppression of dilation and the corresponding reduction in undrained cyclic resistance (Idriss and Boulanger 2008). Previous investigations of the effect of σ'_{v0} on the cyclic resistance of granular soils have been conducted using undrained stress-controlled cyclic laboratory tests (Seed 1983; Seed and Harder 1990; Harder and Boulanger 1997; Vaid and Thomas 1995; Vaid and Sivathayalan 1996; Hynes and Olsen 1999) to build a body of experimental data to inform trends in K_σ with σ'_{v0} and adjustments to the cyclic resistance computed using penetration test–based liquefaction triggering procedures. The understanding of the effect of σ'_{v0} on the cyclic response of natural silts remains poor in comparison.

Wijewickreme et al. (2005) investigated the effect of vertical effective consolidation stress, σ'_{vc}, on the cyclic resistance of normally consolidated (NC) intact and reconstituted laterite tailings and copper–gold–zinc tailings classified as nonplastic and low-plasticity silt (ML) per the Unified Soil Classification System (USCS), with a plasticity index (PI) of 0, 2, and 12 for σ'_{vc} ranging from 100 to 460 kPa. The laterite tailings exhibited densification-driven dilative tendencies which outweighed the increase in contractive tendency associated with greater σ'_{vc}. For the case of the copper–gold–zinc tailings, the cyclic resistance ratio (CRR) was found to be insensitive to the initial density and σ'_{vc}. Sanin and Wijewickreme (2006) reported that the cyclic resistance of intact Fraser River Delta silt [classified as ML, with PI = 4 and overconsolidation ratio (OCR) = 1] was insensitive to the variation in σ'_{vc} over the range 85–200 kPa. However, the effect of damage to the natural soil fabric and the increased density resulting from increased σ'_{vc} was not assessed separately. Verma and Wijewickreme (2018) noted insensitivity of the cyclic resistance to σ'_{vc} for intact, low-plasticity NC Fraser River silt (classified as ML, with PI = 8–9) over the range 400–1,000 kPa, whereas Soysa and Wijewickreme (2015) concluded that the cyclic resistance of intact, high-plasticity NC Fraser River silt (classified as MH; PI = 34) decreased with increases in σ'_{vc} due to breakdown of the natural soil fabric.

Based on the results of previous studies, a systematic assessment of the sensitivity of the cyclic resistance of silts with different plasticity to σ'_{vc} is needed. This study focused on assessing the effects of σ'_{vc} on the cyclic response of several silts obtained from the Willamette Valley in Oregon. These silts vary from nonplastic to slightly plastic. Tests were performed on both intact and reconstituted specimens to assess the influence of soil fabric on material response.

Soil Characterization and Laboratory Testing Program

Characterization of Silt Specimens

A series of laboratory tests was performed on intact normally consolidated (NC) and overconsolidated (OC) and reconstituted NC specimens of nonplastic to high-plasticity silt deposits from Sites E and F described by Stuedlein et al. (2023b). Intact samples were retrieved in accordance with ASTM D1587 (ASTM 2015) from depths ranging from 9.4 to 10 m and from 11.4 to 12 m at Site E (denoted E-3 and E-5, respectively) (Table 1) and from 6.3 to

[1]Geotechnical Engineer, Jacobs Engineering Group, 2020 SW 4th Ave., Suite 300, Portland, OR 972011.

[2]Research Associate, School of Civil and Construction Engineering, Oregon State Univ., 101 Kearney Hall, Corvallis, OR 97331.

[3]Professor, School of Civil and Construction Engineering, Oregon State Univ., 101 Kearney Hall, Corvallis, OR 97331 (corresponding author). ORCID: https://orcid.org/0000-0002-6265-9906. Email: armin.stuedlein@oregonstate.edu

[4]Professor, School of Civil and Construction Engineering, Oregon State Univ., 101 Kearney Hall, Corvallis, OR 97331. ORCID: https://orcid.org/0000-0002-8457-7602

Note. This manuscript was submitted on September 18, 2022; approved on August 2, 2023; published online on September 27, 2023. Discussion period open until February 27, 2024; separate discussions must be submitted for individual papers. This technical note is part of the ***Journal of Geotechnical and Geoenvironmental Engineering***, © ASCE, ISSN 1090-0241.

Table 1. Test parameters and summary of test results of constant-volume, stress-controlled cyclic tests for Site E and F specimens

Test site	Test ID	Vertical effective consolidation stress, σ'_{vc} (kPa)	OCR	Plasticity index, PI	Void ratio, e_c	Average void ratio, $e_{c,\mathrm{AVG}}$	Cyclic stress ratio, CSR	$N_{\gamma=3\%}$	$N_{\gamma=3.75\%}$	$N_{\max}$	$r_{u,\max}$ (%)
					Intact specimens						
E	E-3-1	107	2.1	24	2.33	2.26	0.31	64.8	216.8	677.1	86
	E-3-2			27	2.30		0.44	0.3	1.3	18.1	79
	E-3-3			27	2.19		0.36	3.7	11.8	160.6	84
	E-3-4			24	2.22		0.33	12.3	37.3	191.1	79
	E-5-1	125	2.2	15	0.99	0.92	0.39	0.7	0.8	6.6	90
	E-5-2				0.94		0.35	0.8	1.7	8.5	90
	E-5-3				0.94		0.35	0.8	1.7	7.6	91
	E-5-4				0.96		0.31	1.7	2.8	13.5	90
	E-5-5				0.68		0.22	161.8	208.8	282.6	96
	E-5-6				1.00		0.26	17.8	25.7	57.6	94
	E-3-14	350	1	15	0.88	0.85	0.21	5.7	7.8	19.3	85
	E-3-15				0.83		0.23	1.7	2.7	9.6	84
	E-3-16				0.85		0.17	62.8	75.8	109.5	91
	E-3-17	600	1	15	0.69	0.65	0.18	3.7	11.8	38.5	82
	E-3-18				0.65		0.19	0.2	1.7	16.6	49
	E-5-11				0.61		0.15	24.8	27.7	39.1	99
F	F-1-1	120	2.6	0	0.84	0.92	0.30	0.7	0.8	3.1	96
	F-1-2				0.95		0.20	54.2	58.2	69.5	96
	F-1-3				0.89		0.24	4.3	5.3	11.6	96
	F-1-4				0.99		0.18	39.2	41.3	54.1	98
	F-1-5				0.91		0.15	705.8	716.8	720.0	96
	F-1-6	350	1	3	0.85	0.87	0.15	675.8	715.5[a]	715.5	84
	F-1-7				0.91		0.20	10.8	17.3	27.6	88
	F-1-8				0.92		0.23	1.2	3.2	13.0	83
	F-1-9				0.81		0.18	10.2	15.2	25.0	95
	F-1-10				0.85		0.18	12.2	17.2	31.6	95
	F-1-13	600	1	3	0.56	0.69	0.13	20.8	81.8	120.5	94
	F-1-14				0.71		0.16	2.8	23.3	52.1	93
	F-1-15				0.79		0.17	0.2	6.2	35.1	90
					Reconstituted specimens						
E	E-3-R1	100	1	21	1.02	1.03	0.27	13.2	17.3	43.1	96
	E-3-R2				1.04		0.30	4.2	6.2	31.0	94
	E-3-R3				1.03		0.24	43.2	47.3	87.2	97
	E-3-R4	350	1	21	0.94	0.98	0.20	47.3	119.3	259.1	88
	E-3-R5				1.02		0.23	8.3	17.3	54.6	85
	E-3-R6				0.93		0.26	0.2	1.8	11.6	77
	E-3-R7				0.97		0.24	0.2	2.2	13.1	77
	E-3-R8				1.03		0.23	1.2	4.2	20.1	81
	E-3-R9	600	1	21	0.85	0.74	0.20	1.3	12.3	47.1	80
	E-3-R10				0.75		0.18	0.2	13.3	25.2	55
	E-3-R11				0.79		0.18	7.8	18.7[a]	18.7	47
	E-3-R12				0.56		0.17	127.3	355.6[a]	355.6	66
F	F-1-R1	100	1	4	0.53	0.54	0.20	22.2	24.2	35.0	100
	F-1-R2				0.53		0.22	4.2	5.2	13.0	98
	F-1-R3				0.54		0.18	99.3	102.3	126.1	100
	F-1-R4	350	1	4	0.54	0.53	0.18	23.3	27.2	42.0	92
	F-1-R5				0.52		0.20	1.2	3.3	15.1	91
	F-1-R6				0.53		0.18	16.3	19.2	29.2	92
	F-1-R7				0.55		0.17	33.3	35.2	43.6	93
	F-1-R8	600	1	4	0.46	0.46	0.15	342.3	423.3	428.7	83
	F-1-R9				0.44		0.18	6.3	19.2	40.5	88
	F-1-R10				0.49		0.21	0.2	3.2	13.5	84

[a]These specimens did not reach the target shear strain amplitude $(\hat{I}^3\mathrm{SA} = 3.75\%)$ for the stated number of loading cycles.

6.9 m at Site F (denoted F-1) (Table 1). Samples were retrieved within mud rotary boreholes using Osterberg piston samplers and specially fabricated thin-walled tubes with specifications similar to those described by Wijewickreme et al. (2019). Sample transportation, extrusion, and mounting of specimens followed the guidelines in ASTM D4220-14 (ASTM 2014), and were explained in detail by Dadashiserej et al. (2022a). Reconstituted specimens were prepared from the samples retrieved from Sites E and F using a slurry deposition method described by Wijewickreme and Sanin (2010), which attempts to replicate the soil fabric developed in fluvial environments (Krage et al. 2020).

The soils from Site E described herein were classified as low-plasticity to high-plasticity silt (ML–MH) per the Unified Soil Classification System, with an average natural water content $w_n = 52\%$, $15 \leq \mathrm{PI} \leq 27$, and fines contents (FC) $\approx 99\%$. Soil samples tested from Site F generally were classified as ML, with average $w_n = 38\%$, $0 \leq \text{PI} \leq 4$, and $\text{FC} \approx 52\%$. Constant-rate-of-strain (CRS) consolidation tests conducted on representative intact specimens indicated OCRs of ~2.2 and 2.6 for Sites E and F, respectively (Stuedlein et al. 2023b).

Experimental Test Procedures

Constant-volume, cyclic direct simple shear (CDSS) tests were conducted using the SSH-100 device described by Dadashiserej et al. (2022b). The test program was performed to investigate the effect of overburden stress (i.e., σ'_{vc}) on the cyclic resistance of saturated silt soils. Intact specimens were consolidated to σ'_{vc} equal to the estimated in situ σ'_{v0} to replicate the existing in situ stress state using the recompression method (Bjerrum and Landva 1966); Stuedlein et al. (2023b) presented details of and justification for the method. Additional cyclic tests were conducted on mechanically consolidated NC intact specimens (MC-NC) by exceeding the in situ preconsolidation stress, σ'_p, and achieving σ'_{vc} of 350 and 600 kPa. Reconstituted NC specimens were consolidated to σ'_{vc} of 100, 350, and 600 kPa to elucidate further the effect of σ'_{vc} on the cyclic resistance of silt soils. Following the completion of primary consolidation and at least one log cycle of secondary compression, specimens were subjected to uniform amplitude sinusoidal shear stress cycles, τ_{cyc}, at selected cyclic stress ratios (CSRs), $\tau_{\text{cyc}}/\sigma'_{vc}$, with a loading frequency of 0.1 Hz to a minimum single amplitude shear strain, γ, of 3.75%. The excess pore-pressure ratio, r_u, for constant-volume CDSS specimens may be interpreted as $r_u = 1 - \sigma'_v/\sigma'_{vc}$ (Dyvik et al. 1987), where σ'_v is the vertical effective stress. Individual specimens are distinguished by a corresponding test designation (e.g., Table 1, Figs. 1–4) which indicates the test site, sample, and test number. For example, Test E-3-15 indicates that the specimen was prepared from soils retrieved from Site E, Sample 3, and was the 15th test conducted for the specified soil sample. Reconstituted specimens are distinguished from intact specimens with the addition of the letter R to the test number in their designations.

There were significant differences in PI and corresponding void ratios, e, for the intact specimens prepared from Sample 3 of Site E and tested at σ'_{v0} (i.e., E-3-1 to E-3-4) relative to those tested at $\sigma'_{vc} > \sigma'_{v0}$ (i.e., E-3-14 to E-3-18) (Table 1). The difference in e resulted from the spatial variability within Sample 3. However, intact specimens prepared from Sample 5 of Site E and tested at σ'_{v0} (E-5-1 to E-5-6) had similar PI and e values, prior to consolidation, as Specimens E-3-14 to E-3-18. Therefore, Specimens E-5-1 to E-5-6, which are tested at σ'_{v0}, were compared with those intact specimens of Site E, Sample 3, tested at $\sigma'_{vc} > \sigma'_{v0}$ (i.e., E-3-14 to E-3-18).

Cyclic Response of Intact and Reconstituted Specimens

Intact Specimens

Fig. 1 presents the cyclic response of intact OC and MC-NC specimens of medium to high plasticity from Site E and nonplastic to low-plasticity specimens of Site F in terms of the normalized shear stress–shear strain (CSR–γ) hysteresis and effective stress paths. The specimens all indicated the cyclic mobility-type response [Figs. 1(b, e, h, k, n, and q)], which is characterized by gradual accumulation of γ and degradation in shear stiffness [Figs. 1(a, d, g, j, m, and p)] without an abrupt loss of strength (Castro and Poulos 1977). With the exception of Specimen E-5-4 [Fig. 1(a)], the specimens exhibited sandlike behavior characterized by inverted S-shape hysteresis loops, and transient near-zero shear stiffness with the maximum cyclic shear stress–normalized minimum tangent shear modulus and cyclic shear stress difference, $G_{\tan,\min}/\tau_{\text{cyc,max}}$ and $\Delta\tau_{\text{cyc}}/\tau_{\text{cyc,max}}$ (Stuedlein et al. 2023b), of approximately 2 or less and 0.55 or less, respectively, and varying degrees of dilation hardening just prior to cyclic stress reversal [Figs. 1(d, g, j, m, and p)]. Although the maximum r_u, $r_{u,\max}$, generally decreased with σ'_{vc} for a given shear strain amplitude [Figs. 1(c, f, i, l, o, and r)], the alternate hysteretic metrics, $G_{\tan,\min}/\tau_{\text{cyc,max}}$ and $\Delta\tau_{\text{cyc}}/\tau_{\text{cyc,max}}$, proposed by Stuedlein et al. (2023b) appear to describe the observed sandlike behavior satisfactorily, the tendency for which seemed to increase with increases in σ'_{vc}. Table 1 summarizes the properties of the specimens and the results of cyclic test program, including the number of loading cycles to reach $\gamma = 3\%$ and 3.75%, $N_{\gamma=3\%}$, $N_{\gamma=3.75\%}$, respectively, the maximum number of loading cycles, $N_{\max}$, and $r_{u,\max}$.

The effect of increased σ'_{vc} on the cyclic resistance for soils retrieved from Sites E and F was interpreted in terms of $N_{\gamma=3\%}$ for consistency with common cyclic failure models [e.g., liquefaction (Boulanger and Idriss 2015), cyclic softening (Boulanger and Idriss 2007), and cyclic failure of silts (Stuedlein et al. 2023a)]. Specimens E-5-4 and E-3-15 each resulted in $N_{\gamma=3\%} = 1.7$ [Figs. 1(a and d)], although OC Specimen E-5-4 ($\text{OCR} = 2.2$, $e = 0.96$) was sheared under $\sigma'_{v0} = \sigma'_{vc} = 125$ kPa and a larger $\text{CSR} = 0.31$, compared with the denser MC-NC Specimen E-3-15 ($\text{OCR} = 1$, $e = 0.83$) sheared under $\sigma'_{vc} = 350$ kPa and $\text{CSR} = 0.23$. The constant-volume, monotonic DSS response for Specimen E-5-M1 ($\text{OCR} = 2.2$, $\text{PI} = 15$) consolidated to $\sigma'_{vc} = 125$ kPa reported by Stuedlein et al. (2023b) indicates that the initial state for this material was contractive and that the excess pore pressure generated at failure was larger than that predicted by critical-state soil mechanics theory assuming parallel normal consolidation (NCL) and critical state (CSL) lines. Thus, a change from a dilative to a contractive tendency is not responsible for the lower cyclic resistance exhibited by Specimen E-3-15. Rather, if the CSL is steeper than the NCL in e–$\log\sigma'_v$ space, lower cyclic resistance results from the destruction of the natural soil fabric associated with yielding (i.e., exceedance of σ'_p) and a presumed increase in the state parameter relative to the less dense OC Specimen E-5-4.

The effect of OCR on the cyclic response of these silts can be removed and separated from other contributing factors by comparing the cyclic resistance of the normally consolidated (MC-NC) specimens E-3-15 ($e = 0.83$) [Figs. 1(d and e)] and E-3-18 ($e = 0.65$) [Figs. 1(g and h)] consolidated to $\sigma'_{vc} = 350$ and 600 kPa, respectively. Although Specimen E-3-15 was subjected to a larger CSR, it resulted in greater cyclic resistance ($N_{\gamma=3\%} = 1.7$) than the denser Specimen E-3-18 ($N_{\gamma=3\%} = 0.2$). This observation highlights the dominant effect of natural fabric destruction due to further increases in σ'_{vc} beyond σ'_p and a possible increase in the state parameter over any beneficial effect resulting from increasing density on cyclic resistance. The differing CSRs, which were selected in order to reliably quantify cyclic resistance under the selected strain-based cyclic failure criterion, prevent direct comparison of dilative tendencies. Similar observations about the effect of increased σ'_{vc} on the cyclic resistance of intact, nonplastic to low-plasticity Site F specimens may be drawn [Figs. 1(n–q)]. However, increased σ'_{vc} resulted in a smaller reduction in cyclic resistance of the low-plasticity Site F specimens than of the high-plasticity Site E specimens, as discussed subsequently. Based on the monotonic responses reported by Stuedlein et al. (2023b) and the cyclic responses presented here, the NCL and CSL for Site E and F specimens are not parallel, they exhibit net contractive responses in their in situ state, and become increasingly contractive upon application of larger σ'_{vc} as dilation is

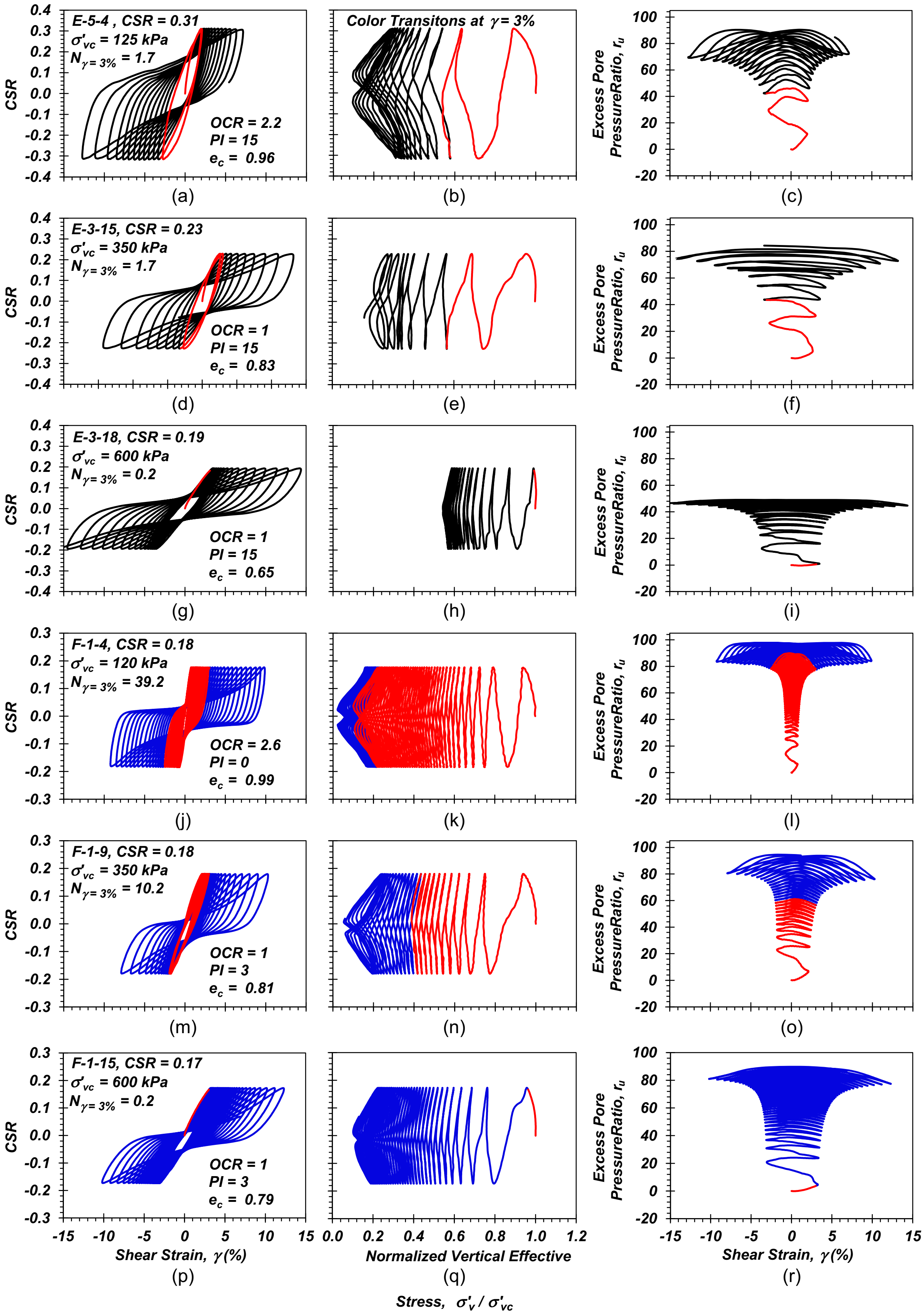

Fig. 1. Cyclic response of intact and MC-NC specimens subjected to stress-controlled cyclic DSS tests: (a, d, and g) Site E, cyclic shear stress–shear strain hysteresis; (b, e, and h) Site E, effective stress paths; (c, f, and i) Site E, variation of excess pore pressure ratio, r_u, with shear strain, γ; (j, m, and p) Site F, cyclic shear stress–shear strain hysteresis; (k, n, and q) Site F, effective stress paths; and (l, o, and r) Site F, variation of excess pore pressure ratio, r_u, with shear strain, γ.

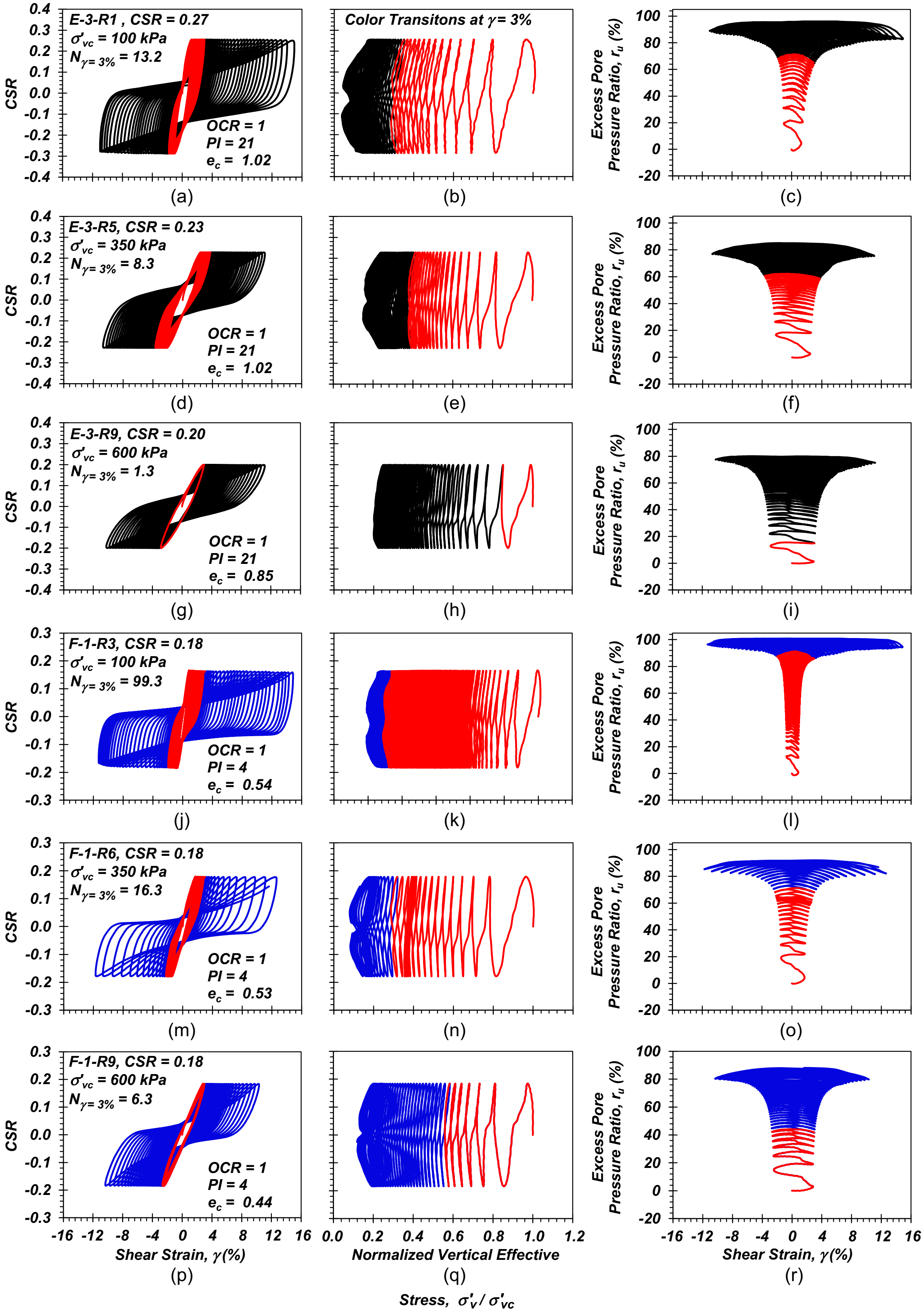

Fig. 2. Cyclic response of NC reconstituted specimens subjected to stress-controlled cyclic DSS tests: (a, d, and g) Site E, cyclic shear stress–shear strain hysteresis; (b, e, and h) Site E, effective stress paths; (c, f, and i) Site E, variation of excess pore pressure ratio, r_u, with shear strain, γ; (j, m, and p) Site F, cyclic shear stress–shear strain hysteresis; (k, n, and q) Site F, effective stress paths; and (l, o, and r) Site F, variation of excess pore pressure ratio, r_u, with shear strain, γ.

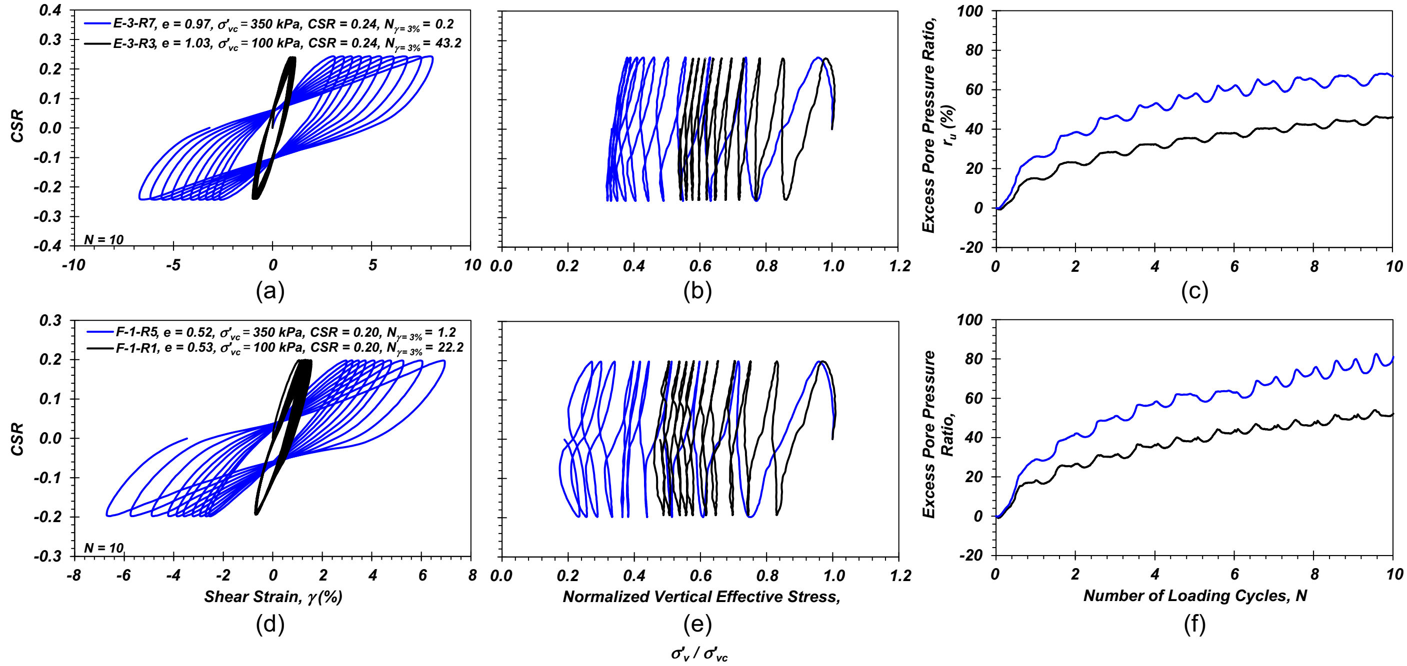

Fig. 3. Examples of the effect of vertical effective consolidation stress, σ'_{vc}, on the cyclic response of reconstituted specimens subjected to stress-controlled cyclic DSS tests: (a) Specimens E-3-R3 and E-3-R7, cyclic shear stress–shear strain (CSR–γ) hysteresis; (b) Specimens E-3-R3 and E-3-R7, effective stress path; (c) Specimens E-3-R3 and E-3-R7, variation of excess pore pressure ratio, r_u, with number of loading cycles, N; (d) Specimens F-1-R1 and F-1-R5, cyclic shear stress–shear strain (CSR–γ) hysteresis; (e) Specimens F-1-R1 and F-1-R5, effective stress path; and (f) Specimens F-1-R1 and F-1-R5, variation of excess pore pressure ratio, r_u, with number of loading cycles, N.

suppressed. In summary, the intact specimens of Sites E and F demonstrate the complexity of isolating the effect of overburden stress on the cyclic resistance of naturally deposited specimens, which necessarily will exhibit varying stress histories and void ratios with depth, dictating different initial states relative to the critical state.

Reconstituted Specimens

Owing to the inability to satisfactorily isolate and quantify the effect of intact versus destructured soil fabric with regard to OCR, state, and potential specimen-to-specimen variability on the cyclic response of natural specimens, the effect of σ'_{vc} was investigated by performing CDSS tests on reconstituted specimens (Table 1). Fig. 2 presents the CSR–γ hysteresis and effective cyclic stress paths for NC reconstituted specimens prepared from the samples of Sites E and F. The reconstituted specimens exhibited cyclic mobility with gradual accumulation of γ and degradation of shear stiffness without abrupt loss of strength. There was a consistent reduction in cyclic resistance with increases in σ'_{vc}. For example, Specimens E-3-R1 ($\sigma'_{vc} = 100$ kPa) and E-3-R5 ($\sigma'_{vc} = 350$ kPa), both with $e = 1.02$ and PI $= 21$, yielded $N_{\gamma=3\%} = 13.2$ and 8.3 for CSRs of 0.27 and 0.23, respectively [Figs. 2(a and d)]. The further reduction in cyclic resistance obtained from the denser Specimen E-3-R9 with $\sigma'_{vc} = 600$ kPa also is evident [Fig. 2(g)], and points solely to the suppression of dilative tendencies as a result of an increase in the contractive state, which overshadows the beneficial effect of densification of these NC specimens. The reconstituted, dense, PI $= 4$ specimens of Site F sheared under the shared CSR of 0.18 confirm the dominant role of suppressed dilative tendencies with increased σ'_{vc} [Figs. 2(j–r)], with greater shear strain amplitudes necessary to trigger dilative tendencies prior to cyclic stress reversal under higher σ'_{vc}. This is more clearly evident in Fig. 3, which presents the results for additional reconstituted test specimens with similar void ratios sheared under identical CSRs. Comparison of the cyclic response of Specimens E-3-R3 and E-3-R7 (Fig. 3) indicates that although Specimen E-3-R7 was slightly denser ($e = 0.97$, $\sigma'_{vc} = 350$ kPa) than Specimen E-3-R3 ($e = 1.03$, $\sigma'_{vc} = 100$ kPa), it exhibited lower shear stiffness [Fig. 3(a)] and a reduced dilative tendency [Fig. 3(b)], and generated greater excess pore pressure for a given cycle of loading [Fig. 3(c)]. Comparison of the low-plasticity reconstituted NC specimens of Site F [Figs. 3(d–f), Table 1], with nearly identical e values, likewise confirms the greater net contractive tendency of such silts under large σ'_{vc}.

Cyclic Resistance and Overburden Correction Factor

Fig. 4 compares the cyclic resistance of the intact and reconstituted nonplastic to high-plasticity Site E and F specimens consolidated to $\sigma'_{vc} = \sim 100$, 350, and 600 kPa in terms of their CRR $- N_{\gamma=3\%}$ relationships to demonstrate succinctly the role σ'_{vc} in CRR. The average CRR of the intact, MC-NC Site E specimens was 20% smaller at $\sigma'_{vc} = 600$ kPa than at 350 kPa over $2 \leq N \leq 25$ [Fig. 4(a)]. Similarly, the average CRR of the intact MC-NC Site F specimens was 26% smaller at $\sigma'_{vc} = 600$ kPa than at 350 kPa over $1 \leq N \leq 21$ [Fig. 4(b)]. The reductions in CRR would have been greater if the specimens had the same e. Although the reconstituted plastic Site E specimens exhibited similar reductions in CRR as σ'_{vc} increased to that observed for the intact specimens, the dense reconstituted low-plasticity Site F specimens exhibited a significantly smaller reduction in CRR as σ'_{vc} increased from 350 to 600 kPa. This likely was due to a greater difference in soil fabric between the intact and reconstituted low-plasticity Site F specimens than for

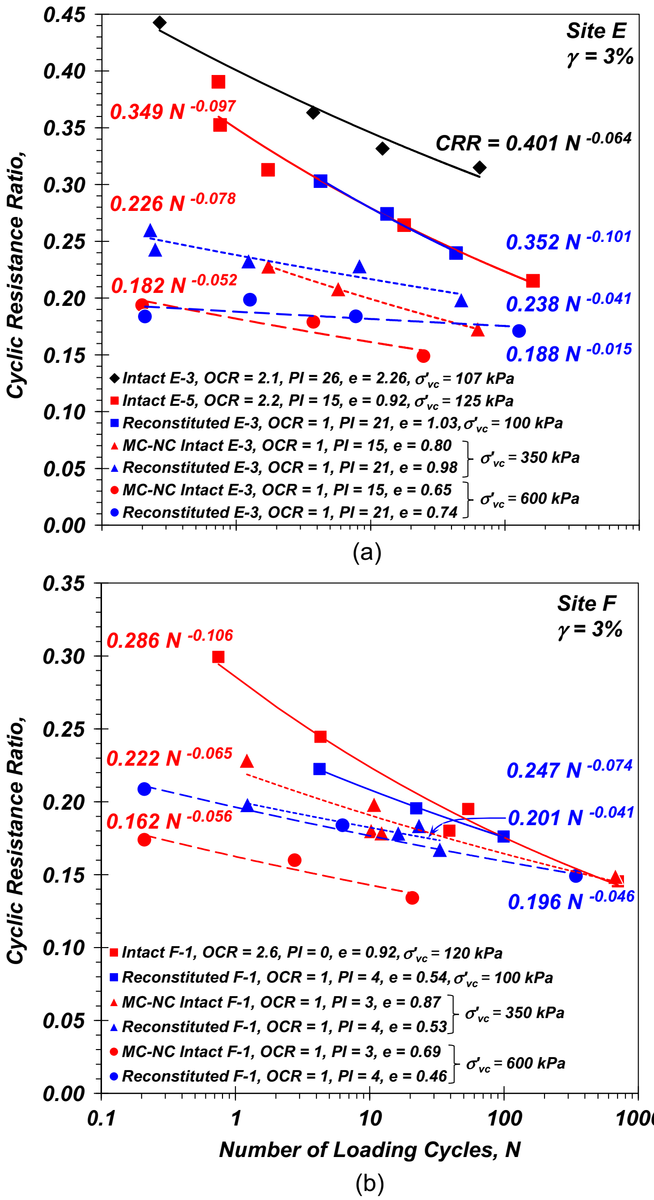

Fig. 4. (a) Cyclic resistance of intact and reconstituted specimens from Sites E and Sites F; and (b) variation of cyclic resistance ratio with number of loading cycles, N, to reach $\gamma = 3\%$.

Site E specimens, which also can be significant for other silts (e.g., Dadashisherej et al. 2022b). Additionally, the increase in density (i.e., from $e = 0.54$ to 0.46 as σ'_{vc} increased from 350 to 600 kPa) for the well-graded Site F specimens may have resulted in a corresponding increases in CRR that offset some of the reduction in CRR due to high σ'_{vc}. The reduction in cyclic resistance of the higher-plasticity Site E specimens generally agreed with findings reported by Soysa and Wijewickreme (2015) and Verma and Wijewickreme (2018) for high-plasticity intact Fraser River silt (PI = 34). However, the CRR of intact NC low-plasticity (PI = 4–9) Fraser River silt specimens was observed to be insensitive to σ'_{vc} over a range of 75–1,000 kPa (Sanin and Wijewickreme 2006; Verma and Wijewickreme 2018). These findings differ from the responses identified from the intact Site E and F soils, perhaps pointing to the role of particle morphology, mineralogy, and/or soil fabric on overburden stress effects.

Furthermore, exponent b describing the slope of the power law $\mathrm{CRR} = aN^{-b}$ was sensitive to the combined effects of stress history and state (i.e., σ'_{vc} and e); intact OC specimens under low σ'_{vc} exhibited steeper slopes (and therefore larger b) than the denser intact MC-NC specimens sheared cyclically under high σ'_{vc}. Such observations are highly relevant for thick and deep deposits of silts, such as those encountered along the banks of the Columbia River west of the Cascades mountain range (e.g., at Longview, WA and Astoria, OR), which exhibit OCRs that decrease with depth. These and similar soils will exhibit substantially differing cyclic resistances in response to near-fault, short-duration crustal (low-N) and distant, long-duration subduction zone (high-N) earthquakes. The sensitivity of b to stress history and state noted for the intact specimens reported herein differs from conclusions about the effect of OCR on b drawn by Stuedlein et al. (2023a). Stuedlein et al. (2023a) statistically analyzed 20 suites of CRR–N curves for intact specimens of nonplastic to plastic silts and determined that the OCR contribution to b was statistically insignificant; however, the majority (70%) of specimens in the database were consolidated to $\sigma'_{v0} = \sigma'_{vc}$ ranging from 100 to 150 kPa, and only 12% of specimens were subjected to larger values of σ'_{vc}. Thus, further research is needed to identify the effect of stress history and state on exponent b and cyclic resistance.

The effect of σ'_{vc} on the cyclic response of the silts investigated in this study may be considered using the overburden correction factor, K_σ (Seed 1983). For level ground, empirical reductions in CRR may be estimated using

$$K_\sigma = \frac{\mathrm{CRR}_{\sigma'_{vc}}}{\mathrm{CRR}_{\sigma'_{vc}=1}} \tag{1}$$

where $\mathrm{CRR}_{\sigma'_{vc}}$ = CRR for soil consolidated under a given σ'_{vc}; and $\mathrm{CRR}_{\sigma'_{vc}=1}$ = cyclic resistance ratio for the same soil consolidated under reference stress $\sigma'_{vc} = 1$ atm (~100 kPa). The CRR used in Eq. (1) is most appropriate for soil with identical characteristics, e.g., fabric, e, OCR, and prior strain history (Montgomery et al. 2014). For reconstituted specimens, K_σ was computed directly using Eq. (1) by normalizing CRR with respect to the CRR of specimens consolidated to $\sigma'_{vc} = 100$ kPa. However, because σ'_{v0} for the intact OC specimens was larger than the reference $\sigma'_{vc} = 100$ kPa (i.e., Site E-5: $\sigma'_{v0} = 125$ kPa; and Site F: $\sigma'_{v0} = 120$ kPa), K_σ was computed using CRRs estimated for $\sigma'_{vc} = 100$ kPa through limited nonlinear interpolation of the observed variation of τ_{cyc} with σ'_{vc} for a given N using curves fitted to the available data through the origin as described by Idriss and Boulanger (2008).

Fig. 5 presents the variation of K_σ with σ'_{vc} and e for intact and reconstituted specimens of Sites E and F for $N_{\gamma=3\%} = 15$ and 30, illustrating the reduction in CRR with increases in σ'_{vc} [Figs. 5(a and c)] and accompanying reductions in e [Figs. 5(b and d)]. Despite a 29% reduction in void ratio for the intact Site E specimens as σ'_{vc} increased from ~100 to 600 kPa, the CRR at $N_{\gamma=3\%} = 30$ decreased from 0.26 to 0.15, with a corresponding $K_\sigma = 0.58$. The comparison of K_σ for the intact specimens of Sites E (PI = 15) and F (PI = 0–3), characterized by similar e and OCR, show that increases in PI lead to larger reduction in cyclic resistance and corresponding K_σ, indicating the role of compressibility on K_σ. This is consistent with the conclusions drawn about the effect of fines content on the compressibility of sand and its stress-dilatancy response reported by Boulanger and Idriss (2004). The K_σ calculated in Fig. 5 for intact specimens may be conservative (i.e., smaller than anticipated) because it includes the coupled detrimental effects of increased σ'_{vc} and the reduction in OCR associated with yielding and destruction of the soil fabric on cyclic resistance when applied to unaltered natural soil deposits (Montgomery et al. 2014).

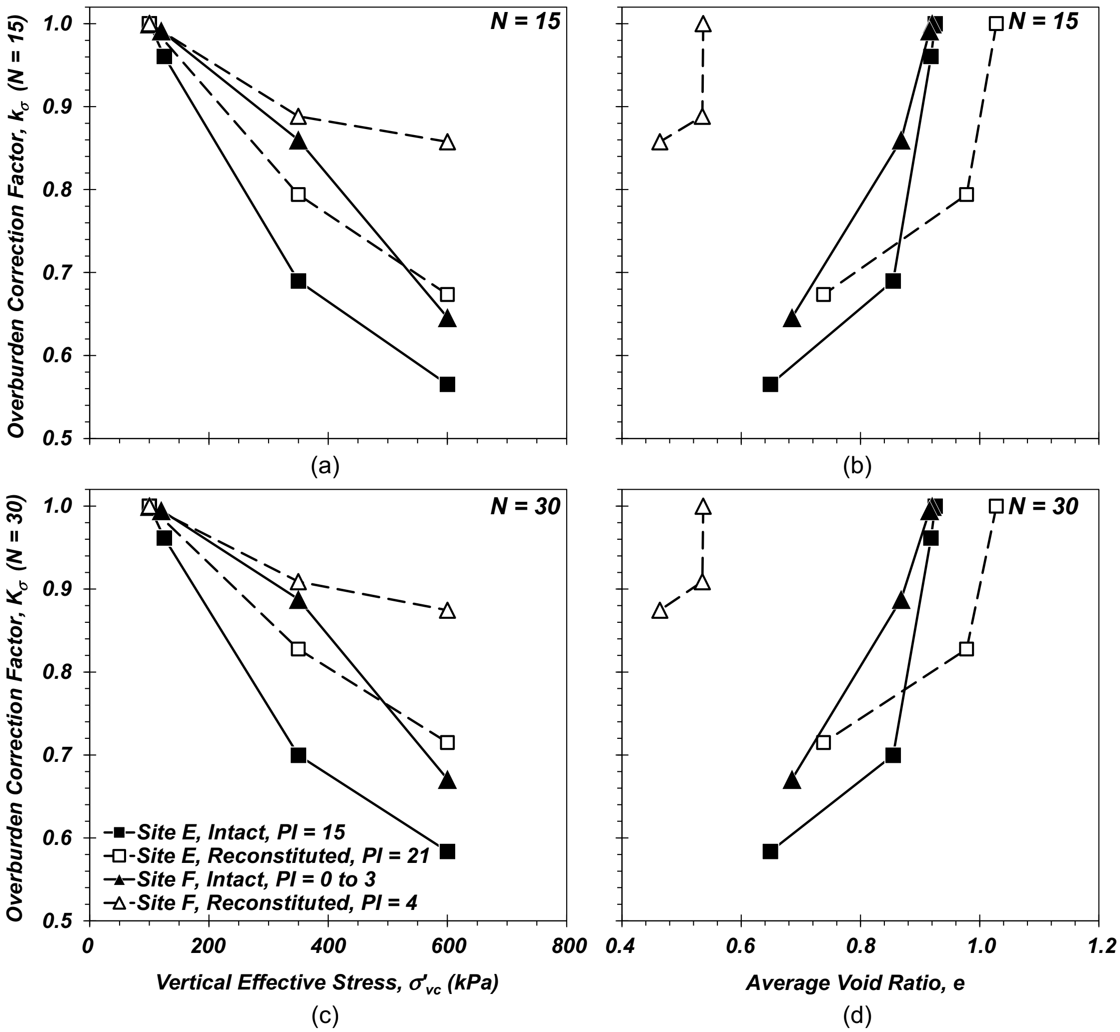

Fig. 5. Variation of the overburden correction factor, K_σ, for Sites E and F with (a) vertical effective stress, σ'_{vc}, for intact and reconstituted specimens, $N = 15$; (b) void ratio, e, for intact and reconstituted specimens, $N = 15$; (c) vertical effective stress, σ'_{vc}, for intact and reconstituted specimens, $N = 30$; and (d) void ratio, e, for intact and reconstituted specimens, $N = 30$.

However, these K_σ values are appropriate for use in assessing the CRR of such deposits in representative scenarios, for example, in the case of the construction of large structures such as dams or following preloading programs leading to the acquisition of NC states, which are common on tracts along the Columbia River. In contrast, the K_σ presented in Fig. 5 for the NC reconstituted specimens may be smaller than expected, most notably for $\sigma'_{vc} > 350$ kPa, because increased σ'_{vc} resulted in significant reductions in e, resulting in partial compensation of the overburden stress effect. However, the effects of differing stress history and soil fabric did not contribute to K_σ for these specimens.

Concluding Remarks

Constant-volume, stress-controlled cyclic direct simple shear (CDSS) tests were conducted to investigate the effect of overburden stress on the cyclic resistance of nonplastic to plastic, overconsolidated (OC) and mechanically consolidated-normally consolidated (MC-NC) intact and NC reconstituted silts. The role of changes in specimen properties such as void ratio, natural soil fabric, and overconsolidation ratio resulting from the increased vertical effective stress, σ'_{vc}, on the reduced cyclic resistance was identified and was found to increase the complexity of the interpretation of results on intact OC and MC-NC specimens. Reconstituted NC specimens tested to reduce the complexity of interpretation clearly identified the role of suppressed dilative tendencies to contribute to the observed reduction in cyclic resistance of the nonplastic to plastic silts evaluated. Specific conclusions of this investigation include:

- Specimens exhibited a reduction in cyclic resistance with increases in σ'_{vc}, despite the accompanying increase in density (i.e., reduction in void ratio).
- The reduction in cyclic resistance of intact specimens is attributed to the dominant effects of yielding of the natural soil fabric, reduction in OCR, and suppression of dilation owing to nonparallel normal consolidation and critical state lines. These effects overshadowed the beneficial effect of increased density.
- The reduction in cyclic resistance of the uniformly prepared, reconstituted NC specimens was associated solely with the suppression of dilative tendencies as σ'_{vc} increased.
- The overburden correction factor, K_σ, depends on PI with a greater reduction with a σ'_{vc} for moderately plastic silts relative to nonplastic to low-plasticity silts, highlighting the role of compressibility on the cyclic resistance of silt.

- The K_σ developed for reconstituted NC specimens may be unconservative due to the role of increased density (i.e., associated with increased σ'_{vc}) on cyclic resistance.
- In contrast, the K_σ developed in this study may be conservative for the intact specimens due to additional factors that contribute to the reduction in cyclic resistance, such as yielding of the soil fabric associated with exceedance of the preconsolidation stress. The representativeness of K_σ depends on whether significant changes in σ'_{vc} are anticipated following construction activity which might result in normally consolidated conditions.

Data Availability Statement

Some or all data, models, or code generated or used during the study are available in a repository online in accordance with funder data retention policies. Specifically, the data described herein are available for public access in the Next Generation Liquefaction Database (https://nextgenerationliquefaction.org/about/index.html).

Acknowledgments

The authors were financially supported in part by the National Science Foundation under Grant CMMI 1663654, the Cascadia Lifeline Program, the Oregon Department of Transportation, and the Pacific Earthquake Engineering Research Center (PEER) through Award 1175-NCTRSA during course of this study. The findings in this study represent the conclusions of the authors and do not necessarily represent the views of the sponsors.

References

ASTM. 2014. *Standard practices for preserving and transporting soil samples*. ASTM D4220. West Conshohocken, PA: ASTM.

ASTM. 2015. *Standard practice for thin-walled tube sampling of fine-grained soils for geotechnical purposes*. ASTM D1587. West Conshohocken, PA: ASTM.

Bjerrum, L., and A. Landva. 1966. "Direct simple-shear tests on a Norwegian quick clay." *Géotechnique* 16 (1): 1–20. https://doi.org/10.1680/geot.1966.16.1.1.

Boulanger, R. W., and I. M. Idriss. 2004. "State normalization of penetration resistance and the effect of overburden stress on liquefaction resistance." In *Proc., 11th Int. Conf. on Soil Dynamics and Earthquake Engineering and 3rd Int. Conf. on Earthquake Geotechnical Engineering*. Berkeley, CA: Univ. of California.

Boulanger, R. W., and I. M. Idriss. 2007. "Evaluation of cyclic softening in silts and clays." *J. Geotech. Geoenviron. Eng.* 133 (6): 641–652. https://doi.org/10.1061/(ASCE)1090-0241(2007)133:6(641).

Boulanger, R. W., and I. M. Idriss. 2015. "Magnitude scaling factors in liquefaction triggering procedures." *Soil Dyn. Earthquake Eng.* 79 (Jun): 296–303. https://doi.org/10.1016/j.soildyn.2015.01.004.

Castro, G., and S. J. Poulos. 1977. "Factors affecting liquefaction and cyclic mobility." *J. Geotech. Geoenviron. Eng.* 103 (6): 501–516. https://doi.org/10.1061/AJGEB6.0000433.

Dadashiserej, A., A. Jana, T. M. Evans, and A. W. Stuedlein. 2022a. "Influence of natural soil fabric on the cyclic resistance of low and high plasticity silts." In *Proc., 12th National Conf. Earthquake Engineering*, 5. Oakland, CA: Earthquake Engineering Research Institute.

Dadashiserej, A., A. Jana, A. W. Stuedlein, and T. M. Evans. 2022b. "Effect of strain history on the monotonic and cyclic response of natural and reconstituted silts." *Soil Dyn. Earthquake Eng.* 160 (Sep): 107329. https://doi.org/10.1016/j.soildyn.2022.107329.

Dyvik, R., S. Lacasse, T. Berre, and B. Raadim. 1987. "Comparison of truly undrained and constant volume direct simple shear tests." *Géotechnique* 37 (1): 3–10. https://doi.org/10.1680/geot.1987.37.1.3.

Harder, L. F., Jr., and R. W. Boulanger. 1997. "Application of KS and KA correction factors." In *Proc., NCEER Workshop on Evaluation of Liquefaction Resistance of Soils*, edited by T. L. Youd and I. M. Idriss, 167–190. Buffalo, NY: Univ. at Buffalo.

Hynes, M. E., and R. Olsen. 1999. "Influence of confining stress on liquefaction resistance." In *Physics and mechanics of soil liquefaction*, edited by P. V. Lade and J. A. Yamamuro, 145–152. Rotterdam, Netherlands: A. A. Balkema.

Idriss, I. M., and R. W. Boulanger. 2008. *Soil liquefaction during earthquakes*. EERI Monograph No. 12. Oakland, CA: Earthquake Engineering Research Institute.

Krage, C. P., A. B. Price, W. G. Lukas, J. T. DeJong, D. J. DeGroot, and R. W. Boulanger. 2020. "Slurry deposition method of low-plasticity intermediate soils for laboratory element testing." *Geotech. Test. J.* 43 (5): 1269–1285.

Montgomery, J., R. W. Boulanger, and L. F. Harder Jr. 2014. "Examination of the K_σ overburden correction factor on liquefaction resistance." *J. Geotech. Geoenviron. Eng.* 140 (12): 04014066. https://doi.org/10.1061/(ASCE)GT.1943-5606.0001172.

Sanin, M., and D. Wijewickreme. 2006. "Influence of initial confining stress on the mechanical response of natural Fraser River Delta silt." In *Proc., 59th Canadian Geotechnical Conf.*, 252–257. Surrey, BC, Canada: Canadian Geotechnical Society.

Seed, H. B. 1983. "Earthquake resistant design of earth dams." In *Proc., Symp. on Seismic Design of Embankments and Caverns*, 41–64. New York: ASCE.

Seed, R. B., and L. F. Harder. 1990. "SPT-based analysis of cyclic pore pressure generation and undrained residual strength." In *Proc., Seed Memorial Symp.*, edited by J. M. Duncan, 351–376. Richmond, BC, Canada: BiTech.

Soysa, A., and D. Wijewickreme. 2015. "Cyclic shear loading response of relatively high-plastic natural fine-grained soil from the Fraser River Delta." In *Proc., 11th Canadian Conf. Earthquake Engineering*. Vancouver, BC: Canadian Association for Earthquake Engineering.

Stuedlein, A. W., A. Dadashiserej, and A. Jana. 2023a. *Estimation of the cyclic resistance of silts and evaluation of cyclic failure during subduction zone earthquakes*. PEER Rep. No. 2023-01. Berkeley, CA: Univ. of California, Berkeley.

Stuedlein, A. W., A. Dadashiserej, A. Jana, and T. M. Evans. 2023b. "On the liquefaction susceptibility and cyclic response of intact nonplastic and plastic silts." *J. Geotech. Geoenviron. Eng.* 149 (1): 04022125. https://doi.org/10.1061/(ASCE)GT.1943-5606.0002935.

Vaid, Y. P., and S. Sivathayalan. 1996. "Static and cyclic liquefaction potential of Fraser Delta sand in simple shear and triaxial tests." *Can. Geotech. J.* 33 (2): 281–289. https://doi.org/10.1139/t96-007.

Vaid, Y. P., and J. Thomas. 1995. "Liquefaction and postliquefaction behavior of sand." *J. Geotech. Eng.* 121 (2): 163–173. https://doi.org/10.1061/(ASCE)0733-9410(1995)121:2(163).

Verma, P., and D. Wijewickreme. 2018. "Effect of high initial effective confining stress on the mechanical response of natural silt." In *Proc., Geotechnical Earthquake Engineering and Soil Dynamics V: Slope Stability and Landslides, Laboratory Testing, and In Situ Testing*, 208–218. Reston, VA: ASCE.

Wijewickreme, D., and M. Sanin. 2010. "Postcyclic reconsolidation strains in low-plastic Fraser River Silt due to dissipation of excess pore-water pressures." *J. Geotech. Geoenviron. Eng.* 136 (10): 1347–1357. https://doi.org/10.1061/(ASCE)GT.1943-5606.0000349.

Wijewickreme, D., M. V. Sanin, and G. R. Greenaway. 2005. "Cyclic shear response of fine-grained mine tailings." *Can. Geotech. J.* 42 (5): 1408–1421. https://doi.org/10.1139/t05-058.

Wijewickreme, D., A. Soysa, and P. Verma. 2019. "Response of natural fine-grained soils for seismic design practice: A collection of research findings from British Columbia, Canada." *Soil Dyn. Earthquake Eng.* 124 (May): 280–296. https://doi.org/10.1016/j.soildyn.2018.04.053.